CONCRETE LIBRARY OF JSCE NO. 14, MARCH 1990

PROPAGATION CHARACTERISTICS OF VIBRATION IN FRESH CONCRETE FROM INTERNAL VIBRATOR

(Rearrangement of a paper in Proceedings of JSCE No.402, Feb. 1989)

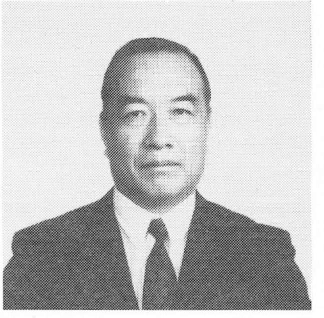

Noriaki IWASAKI　　Nobuyoshi SAKAMOTO

SYNOPSIS

Vibration in fresh concrete propagating two-dimensionally from an internal vibrator was investigated. A theoretical equation which represents the amplitude of displacement or acceleration at an arbitrary point has proposed. A series of experiments to verify the theory was conducted and the equation was proved to provide a reliable basis even for predicting the effects of reflected waves from the surfaces of the form. A method for estimating two parameters essential to a complete description of the vibration; transmission ratio of acceleration between vibrator and concrete and attenuation coefficient of acceleration during propagation; has been offered.

N. IWASAKI is a professor of civil engineering at Toyo University, Saitama, Japan. He took his doctorate in engineering at Tokyo University in 1962. His research interests include vibratory consolidation of concrete, and preplaced aggregate concrete. He was awarded a JSCE prize (the Yoshida prize) in 1986 for a research in preplaced aggregate concrete. He is a member of JSCE and JCI.

N. SAKAMOTO is an associate professor at Toyo University. He took the degree of Master of Engineering at Toyo University in 1969. His research interests include the compaction of concrete by internal vibrator and its improvement. He is a member of JSCE and JCI.

---

1. INTRODUCTION

A large number of investigations relevant to the effectiveness of concrete vibrators have been made in the past. As for the internal vibrator, the relations between its action on fresh concrete and characteristics such as frequency, amplitude, acceleration, and diameter have often been dealt with. In spite of a great deal of data, however, there has been little progress in understanding the basic phenomina because of the complexity of the factors influencing the compaction results. Therefore, it is theoretical basis that is now most required, and it may involve the theories of, (1) the capacity of vibrator, (2) the transmission from vibrator to fresh concrete and propagation of vibration, and (3) the behavior of concrete during vibration. This research is concerned mainly with (2), which is considered to be essential to estimate the range of the effective action of a vibrator, and the object of the research is to establish methods for predicting the intensity distribution of vibration as well as for analysing the experimental results theoretically.

In relation to the damping of the vibration in fresh concrete, the following formula is known.

$$s_2 = s_1 \sqrt{\frac{R_1}{R_2}}\, e^{-\frac{\Omega}{2}(R_2 - R_1)} \cdots\cdots (1)$$

in which s_1, s_2=the amplituds at the respective distances of R_1 and R_2, Ω= coefficient of damping. Bergstrom has reported that the variation in the amplitude of displacement with the distance from the vibrator is closely similar to the variation in pressure, but that it cannot be used directly for estimating the degree of compaction (1). Kamiyama, et al. measured the pressure during vibration, and obtained the following formulas

$$Y = \frac{129}{\sqrt{X}} e^{-0.017X} \quad \text{(ordinary concrete)} \quad \cdots\cdots (2)$$

$$Y = \frac{175}{\sqrt{X}} e^{-0.027X} \quad \text{(lightweight concrete)} \quad \cdots\cdots (3)$$

in which X=radial distance from the surface of the vibrator (cm), and Y=relative acceleration (2). Though these formulas indicate the reduction of vibration with the distance from the vibrator, they can give almost no information about the influences of the reflected waves by the form or reinforcing steel bars. Murata suggested the relation

$$a = a_0 \exp(-\beta x) \sin \omega (t - x/c) \cdots\cdots (4)$$

in which a=acceleration, a_0=acceleration of vibration source, x=distance, β= attenuation coefficient, c=velocity of wave of propagation, ω=angular velocity, and t=time (3). This still remains one-dimensional.

In this research, a function which describes the vibration generated in fresh concrete by the internal vibrator has been derived from the considerations of the vibration mechanism of the vibrator, the geometrical energy distribution, and the energy absorption due to the internal friction of concrete. Then, to verify its validity, two-dimensional experiments have been made associated with the parameters included in the function such as frequency of the vibrator, velocity of wave of propagation, transmission rate and attenuation coefficient of acceleration. Further, combined waves generated by a twin type vibrator have been analysed and tested to assess the applicability of the proposed wave function to the case that the interference may occur.

2. FUNCTION OF TWO-DIMENSIONAL WAVE PROPAGATING FROM AN INTERNAL VIBRATOR

Vibratory motion of internal vibrator is secured mostly by means of an unbalanced eccentric weight rotating in the vibration head. Fig. 1 shows a rough sketch of the vibrating part. For the purpose of two-dimensional analysis, x, y coordinates are taken as Fig. 2 with the origin at the center of the vibrator head inserted in the concrete vertically. Time is measured from a certain instant at which the gravity centroid of the rotating unbalanced axle comes right on the x-axis in the positive direction. Then, the waves which propagate horizontally from the surface of the vibrator may be dealt with as follows.

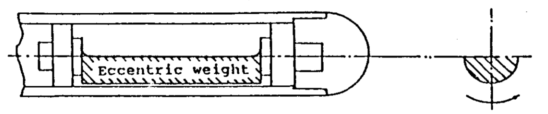

Fig. 1 Sketch of the vibrating part of an eccentric weight type internal vibrator.

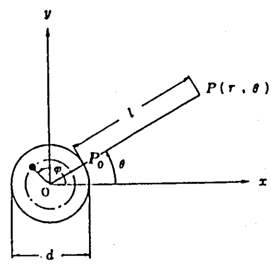

Fig. 2

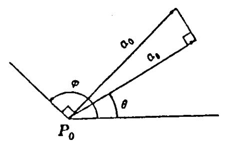

Fig. 3

If the present time is t (sec), the wave front which passes just point P with coordinates (r, θ) is supposed to have been emitted from the surface of the vibrator at the time t_s (sec) written as

$$t_s = t - l/c \qquad (5)$$

in which l=radial distance from the surface of the vibrator to point P, c=velocity of wave of propagation in fresh concrete. Then, the angle between the x-axis and the gravity centroid of the unbalanced eccentric weight axle φ is

$$\varphi = \omega t_s = \omega\left\{t - \frac{1}{c}\left(r - \frac{d}{2}\right)\right\} \qquad (6)$$

in which ω=angular velocity of rotation of the axle (s^{-1}), r=distance from the origin, d=diameter of the vibrator head. Because the phase of the displacement of the head is $\pi/2$ behind that of the motion of the gravity centroid, if the displacement amplitude of the concrete at the surface of the vibrating head is designated as a_0, its component in θ-direction a_θ (cf. Fig. 3) will be

$$a_\theta = a_0 \cos\left(\varphi - \theta - \frac{\pi}{2}\right)$$
$$= a_0 \sin\left\{\omega t - \frac{\omega}{c}\left(r - \frac{d}{2}\right) - \theta\right\} \qquad (7)$$

As for the amplitude, two factors are to be taken into account. Supposing the energy of vibration is not absorbed by a medium, the total energy passing through the cylindrical surface with a radius r and unit height during a period of vibration is equal to that transmitted from the head to the surrounding concrete of unit thickness during the same period. Then, the ratio of the displacement amplitude at the cylindrical surface to that transmitted from the vibrator to the concrete is $\sqrt{d/2r}$, because the energy of vibration is proportional to the square of amplitude. With regard to the energy absorption due to the internal friction of the medium, it is well known that the damping is exponential (2),(3),(4). Taking these two effects into consideration, the equation of the vibration at point P becomes

$$a_{r\theta}=a_0\sqrt{\frac{d}{2r}}\,e^{-\beta\left(r-\frac{d}{2}\right)}\sin\left\{\omega t-\frac{\omega}{c}\left(r-\frac{d}{2}\right)-\theta\right\}$$

$$=a_0\sqrt{\frac{d}{2r}}\,e^{-\beta\left(r-\frac{d}{2}\right)}\sin\left\{2\pi ft-\frac{2\pi f}{c}\left(r-\frac{d}{2}\right)-\theta\right\}\quad\cdots\cdots(8)$$

in which β=attenuation coefficient (cm^{-1}), f=frequency ($=\omega/2\pi$, Hz). Then the acceleration at point P is

$$\alpha=\frac{\partial^2 a_{r\theta}}{\partial t^2}=-a_{r\theta}\omega^2$$

$$=-\alpha_0\sqrt{\frac{d}{2r}}\,e^{-\beta\left(r-\frac{d}{2}\right)}\sin\left\{\omega t-\frac{\omega}{c}\left(r-\frac{d}{2}\right)-\theta\right\}\quad\cdots\cdots(9)$$

in which α_0=amplitude of acceleration of concrete at $r=d/2$, ($=a_0\omega^2$). Consequently if time t (sec) is measured from an instant at which the gravity centroid of the rotating axle comes right on the x-axis in the negative direction, Eq. (9) will be identical to Eq. (8), in that case the letter 'a' means the amplitude of acceleration of concrete.

3. VELOCITY AND FREQUENCY OF THE WAVE IN FRESH CONCRETE

3.1 Description of Experiments

To examine the velocity of wave of propagation c and the frequency f included in Eq. (8), accelerations in fresh concrete slabs at eight points along a straight line from the vibrator were recorded by an electro-magnetic oscillograph. The slab form used and the points measured are illustrated in Fig. 4. The bottom and walls of the form were doubly lined with rubber and styrol foam to ensure freedom from disturbance caused by reflection. Concrete was uniformly spread to half the slab thickness, and the accelerometers were placed and oriented to the point at which the vibrator was to be inserted. Then, the concrete for the upper half of the slab was carefully placed to the total thickness of the slab (=25 cm). The properties of the concrete used are shown in Table 1. The accelerometers embedded in the concretes were water-proof strain gauge type inverters with a maximum range of 20 G, resonance frequency of 530 Hz, dimensions of 18×18×24 mm, and mass of 40 g. The vibrator employed in the experiments was a flexible shaft internal vibrator. Its frequency of vibration was variable over a wide range by means of an inverter and the vibrating head was exchangeable.

Table 1 Properties of concrete.

Concrete	Slump (cm)	Air (%)	W/C (%)	s/a (%)	W (kg)	Max size (mm)
Plain	5.0	2.0	55.0	46.0	166.0	20
AE		7.0		43.5	135.0	

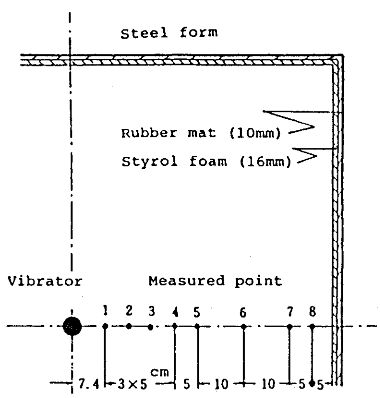

Fig. 4 Slab form used in the experiments and the points where the accelerations were measured.

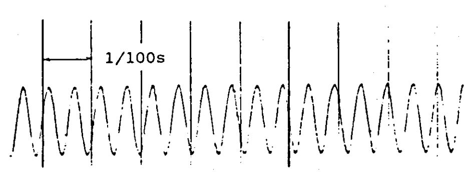

Fig. 5 Vibration of the internal vibrator inserted in fresh concrete.

In all tests the head was fixed to the one with a diameter of 40 mm, and the frequency was 200 Hz. Fig. 5 is an example of its vibration operating in the concrete. It was measured by an accelerometer with a maximum range of 200 G directly attached to the head. The measurement of the acceleration in the concrete was made simultaneously for all the points from immediately after inserting to 30 sec at regular intervals of 5 sec. The running speed of the recording paper was 100 m/sec. Fig. 6 shows a typical result.

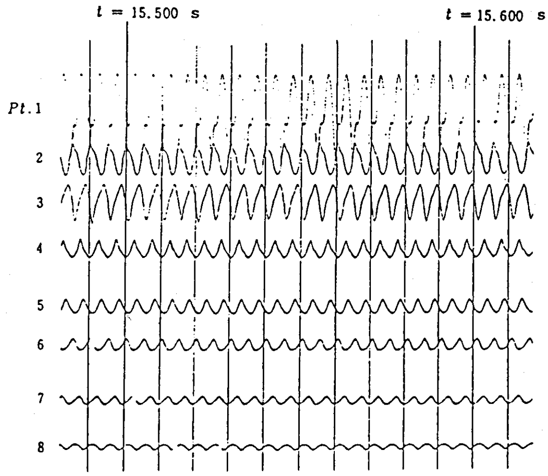

Fig. 6 Typical waves recorded by an oscillograph.

3.2 Results and Considerations

The velocity of wave can be obtained from the differences of the peak time and the distance between two points, and the frequency is the reciprocal of peak-to-peak time. The wave velocities in Table 2 have been calculated between Pt.4 and Pts. 5, 6, and 7. As is seen in the table, they are in the range from 38.5 m/sec to 55.6 m/sec, except for the value for Pt. 6 of Test No. 1, and the mean is 49.7 m/sec.

Table 2 Experimental results of frequency and wave velocity.

Concrete			Plain					AE				
Test No.	Measured point	Distance from the Pt.4(cm)	Peak time (s)	Time lag (ms)	Velocity between Pt.4(m/s)	Period of 20 peaks (s)	Frequency (Hz)	Peak time (s)	Time lag (ms)	Velocity between Pt.4(m/s)	Period of 20 peaks (s)	Frequency (Hz)
1	4	0	0.7800	0	-	0.1012	197.6	0.8400	0	-	0.1036	193.1
	5	5	0.7809	0.9	55.6	0.1013	197.4	0.8422	2.1	23.8	0.1035	193.2
	6	15	0.7815	1.5	100.0	0.1013	197.4	0.8456	5.6	26.8	0.1039	192.5
	7	25	0.7850	5.0	50.0	0.1012	197.6	0.8500	10.0	25.0	0.1032	193.8
2	4	0	5.6800	0	-	0.1011	197.8	5.6100	0	-	0.1052	190.1
	5	5	5.6813	1.3	38.5	0.1011	197.8	5.6122	2.2	22.7	0.1056	189.4
	6	15	5.6832	3.2	46.9	0.1011	197.8	5.6158	5.8	25.9	0.1058	189.0
	7	25	5.6855	5.5	45.5	0.1010	198.0	5.6200	10.0	25.0	0.1057	189.2
3	4	0	10.4300	0	-	0.1005	199.0	10.7100	0	-	0.1051	189.9
	5	5	10.4309	0.9	55.6	0.1005	199.0	10.7122	2.2	22.7	0.1058	189.0
	6	15	10.4330	3.0	50.0	0.1005	199.0	10.7157	5.7	26.3	0.1058	189.0
	7	25	10.4350	5.0	50.0	0.1006	198.8	10.7198	9.8	25.5	0.1052	190.1
4	4	0	15.5530	0	-	0.1007	198.6	15.5200	0	-	0.1050	190.5
	5	5	15.5540	1.0	50.0	0.1007	198.6	15.5216	1.6	31.3	0.1050	190.5
	6	15	15.5561	3.1	48.4	0.1006	198.8	15.5255	5.5	27.3	0.1050	190.5
	7	25	15.5580	5.0	50.0	0.1006	198.8	15.5289	8.9	28.1	0.1050	190.5
5	4	0	20.8000	0	-	0.1003	199.4	20.5800	0	-	0.1050	190.5
	5	5	20.8010	1.0	50.0	0.1003	199.4	*	-	-	*	-
	6	15	20.8030	3.0	50.0	0.1005	199.0	20.5856	5.6	26.8	0.1052	190.1
	7	25	20.8050	5.0	50.0	0.1005	199.0	20.5890	9.0	27.8	0.1050	190.5
6	4	0	25.7590	0	-	0.1000	200.0	25.5500	0	-	0.1050	190.5
	5	5	25.7600	1.0	50.0	0.1005	199.0	*	-	-	*	-
	6	15	25.7620	3.0	50.0	0.1005	199.0	25.5558	5.8	25.9	0.1047	191.0
	7	25	25.7640	5.0	50.0	0.1005	199.0	25.5591	9.1	27.5	0.1047	191.0
7	4	0	30.7000	0	-	0.1009	198.2	30.5300	0	-	0.1042	191.9
	5	5	30.7009	0.9	55.6	0.1009	198.2	*	-	-	*	-
	6	15	30.7031	3.1	48.4	0.1010	198.0	30.5355	5.5	27.3	0.1047	191.0
	7	25	30.7051	5.1	49.0	0.1011	197.8	30.5390	9.0	27.8	0.1043	191.8

* Impossible to obtain the accurate readings because of the disturbed peaks

The data for the other points are not listed, for Pts. 1, 2, and 3 were so close to the vibrator that the characteristics of concrete might change with the advance of compaction. Especially at Pt. 1, the influence of noise was observed. As this sort of disturbance of vibration was not recorded in the tests for mortar, it was probably caused by the direct contacts of coarse aggregates to the vibrator. On the other hand, at Pt. 8 the amplitude of vibration was comparatively small and the peaks were not sharp. In the case of AE cocrete, the wave velocity was estimated to be 26.3 m/sec.

From the application of the theory for longitudinal waves in a fluid containing air bubbles, the velocity of wave through fresh concrete is derived as

$$c=\sqrt{\frac{1}{A(1-A)}\cdot\frac{K_A}{\rho}} \quad \cdots\cdots(10)$$

in which A=air content (volume ratio), ρ=density of the fresh concrete containing no air bubbles (kg/m^3), K_A=bulk modulus of elasticity of air (1.43×10^5 N/m^2). Assuming ρ=2,430 kg/m^3, A=0.02 for ordinary concrete and 0.07 for AE concrete, Eq. (10) gives c=54.8 m/sec and 30.1 m/sec, respectively. As these values agree reasonably with the test results, Eq. (10) may be applicable to estimate the velocity of wave of propagation in fresh concrete.

As to the frequency, it does not vary with different measured points as seen in the table, while a tendency slightly to decrease with the test number is also noticed. This indicates that the frequency of the vibration in fresh concrete is kept constant regardless of the position, and that it has a slight trend to decrease with the time of vibration which may probably be attributed to the reduction of the frequency of the vibrator itself. Similar tendency is seen in the case of AE concrete.

4. WAVE FRONT OF VIBRATION FROM AN INTERNAL VIBRATOR

4.1 Wave Front of Vibration Described by Equation (8)

A shape of wave front is obtained as a locus of the points which have an identical phase of vibration, so, at a given time t, a point which is at its maximum acceleration should satisfy the equation

$$\sin\left\{2\pi ft-\frac{2\pi f}{c}\left(r-\frac{d}{2}\right)-\theta\right\}=1 \quad \cdots\cdots(11)$$

Consequently, the relation between r and θ is

$$r=\frac{d}{2}+ct-\frac{c}{2\pi f}\left(\theta+\frac{\pi}{2}\right) \quad \cdots\cdots(12)$$

This equation represents a swirly curve. The left term of Eq. (11) can be transformed into

$$\begin{aligned}&\sin\left\{2\pi ft-\frac{2\pi f}{c}\left(r-\frac{d}{2}\right)-\theta\right\}\\ &=\sin\left\{2\pi ft-\frac{2\pi f}{c}\left(r-\frac{d}{2}+\frac{c}{f}\right)-\theta+2\pi\right\}\\ &=\sin\left\{2\pi ft-\frac{2\pi f}{c}\left(r-\frac{d}{2}+\frac{c}{f}\right)-\theta\right\}\end{aligned}$$

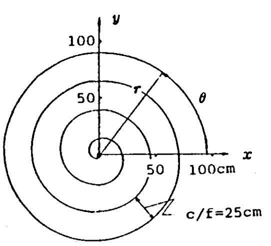

Fig. 7 Calculated wave front propagating from the vibrator.

So, the swirly wave front has regular intervals of c/f. For example, with the values d=40 mm, f=200 Hz, c=50 m/sec, and t=0.02 sec, Eq.(12) becomes $r=95.8-12.5\,\theta/\pi$. Fig. 7 is an illustration of this equation.

4.2 Experiments on Wave Front and Considerations

To substantiate the above remarks, the measurement of accelerations was made simultaneously at seven points on a circle (Fig. 8). The results for the radii of 15 cm and 25 cm are given in Table 3. As the measured points are equidistant from the vibrator, the difference in peak time is to be attributed to the rotating motion of the eccentric weight axle, as long as the velocity of wave differs little with the direction of travelling. And if it does so, the time lag will be

$$\Delta t=\frac{\Delta\theta}{\omega}=\frac{\Delta\theta}{2\pi f}\cdots\cdots\cdots\cdots\cdots\cdots\cdots\cdots\cdots\cdots\cdots\cdots(13)$$

Table 3 Differences in peak time at the points on one circle.

No.	Pt	r (cm) / θ	15: Peak time (s)	15: Time lag (ms)	15: Frequency (Hz)	15: t-lag theory (ms)	25: Peak time (s)	25: Time lag (ms)	25: Frequency (Hz)	25: t-lag theory (ms)
1	1	0	0.7000	0		0	0.5100	0		0
	2	$-\pi/2$	0.7020	2.0		1.27	0.5113	1.3		1.28
	3	$-\pi$	0.7030	3.0		2.54	0.5128	2.8		2.57
	4	$-5\pi/4$	0.7015	1.5	197.0	3.17	0.5110	1.0	194.9	3.21
	5	$-3\pi/2$	0.7018	1.8		3.80	0.5115	1.5		3.85
	6	$-5\pi/3$	0.7045	4.5		4.23	0.5148	4.8		4.28
	7	$-11\pi/6$	0.7052	5.2		4.65	0.5159	5.9		4.70
2	1	0	0.9800	0		0	0.6900	0		0
	2	$-\pi/2$	0.9816	1.6		1.27	0.6914	1.4		1.29
	3	$-\pi$	0.9828	2.8		2.54	0.6929	2.9		2.58
	4	$-5\pi/4$	0.9815	1.5	196.5	3.18	0.6911	1.1	194.0	3.22
	5	$-3\pi/2$	0.9818	1.8		3.82	0.6915	1.5		3.87
	6	$-5\pi/3$	0.9845	4.5		4.24	0.6949	4.9		4.30
	7	$-11\pi/6$	0.9850	5.0		4.66	0.6960	6.0		4.73
3	1	0	5.4900	0		0	5.4700	0		0
	2	$-\pi/2$	5.4918	1.8		1.30	5.4720	2.0		1.31
	3	$-\pi$	5.4930	3.0		2.60	5.4730	3.0		2.63
	4	$-5\pi/4$	5.4907	0.7	192.3	3.25	5.4712	1.2	190.3	3.28
	5	$-3\pi/2$	*	-		3.90	5.4713	1.3		3.94
	6	$-5\pi/3$	5.4940	4.0		4.33	5.4748	4.8		4.38
	7	$-11\pi/6$	5.4952	5.2		4.77	5.4759	5.9		4.82
4	1	0	10.7300	0		0	10.53	0		0
	2	$-\pi/2$	10.7318	1.8		1.30	10.5317	1.7		1.31
	3	$-\pi$	10.7326	2.6		2.61	10.5324	2.4		2.61
	4	$-5\pi/4$	10.7316	1.6	191.4	3.27	10.5308	0.8	191.4	3.27
	5	$-3\pi/2$	*	-		3.92	10.5309	0.9		3.92
	6	$-5\pi/3$	10.7342	4.2		4.35	10.5341	4.1		4.35
	7	$-11\pi/6$	10.7352	5.2		4.79	10.5351	5.1		4.79
5	1	0	15.1000	0		0	15.5400	0		0
	2	$-\pi/2$	15.1020	2.0		1.31	15.5424	2.4		1.31
	3	$-\pi$	15.1026	2.6		2.62	15.5430	3.0		2.62
	4	$-5\pi/4$	15.1010	1.0	190.7	3.28	15.5417	1.7	190.7	3.28
	5	$-3\pi/2$	15.1010	1.0		3.93	15.5412	1.2		3.93
	6	$-5\pi/3$	15.1044	4.4		4.37	15.5442	4.2		4.37
	7	$-11\pi/6$	15.1051	5.1		4.81	15.5452	5.2		4.81
Ave.	1	0		0		0		0		0
	2	$-\pi/2$		1.84		1.29		1.76		1.30
	3	$-\pi$		2.80		2.58		2.82		2.60
	4	$-5\pi/4$		1.26	193.6	3.23		1.16	192.3	3.25
	5	$-3\pi/2$		1.53		3.87		1.28		3.90
	6	$-5\pi/3$		4.32		4.30		4.56		4.34
	7	$-11\pi/6$		5.14		4.74		5.62		4.77

* Impossible to obtain the accurate readings because of the disturbed peaks

The results calculated by Eq. (13) are also given in the table. Fig. 9 shows the differences in peak time measured between Pt. 1 and the other points in comparison with the calculated results by Eq. (13) in the case of r=15 cm. The experimental values for Pts. 2, 3, 6, and 7 agree satisfactorily with calculations, though the results for Pts. 4 and 5 deviate from the calculated values. These deviations are recognized irrespective of the test number or the time of vibration, and similar results are noticed in the test for the radius of 25 cm with another slab employing the same measuring instruments. For these reasons, there probably were something defective in the measuring channels for Pts. 4 and 5.

As seen in the columns of peak time in Table 3, at the peak time of Pt. 1 the other points remain before peaks. The positions of the peaks are supposed to exist on the lines connecting each point to the origin and can be estimated from the time lag Δt and the velocity of wave c, as $r=15-c\Delta t$ or $r=25-c\Delta t$.

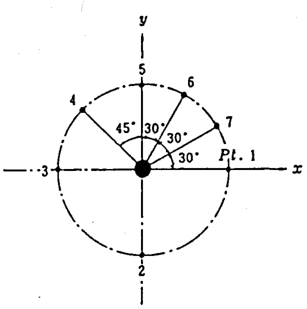

Fig. 8 Measured points all on one circle.

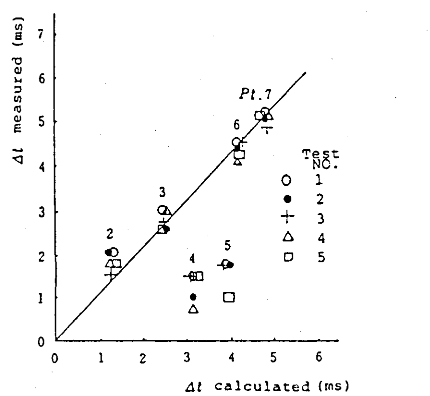

Fig. 9 Comparison of the peak time lags obtained by experiments and theory.

In Table 4, the values of r in the columns of 'Experiment' have been obtained by use of the measured time lags.

While, from Eq. (8), at the peak time

$$\omega t-\frac{\omega}{c}\left(r-\frac{d}{2}\right)-\theta=\frac{\pi}{2} \quad \cdots\cdots(14)$$

By substituting the measured values; d=4 cm, c=26.3 m/sec, f=194 Hz or $\omega=2\pi f=-388\pi$ (the minus sign is due to the clockwise rotation of the eccentric weight axle), θ=0, r=15 cm; time t is calculated as 0.00365 sec. Thus the relations between r and θ become

$$r=15+2.16\theta \quad \cdots\cdots(15)$$

$$r=25+2.16\theta \quad \cdots\cdots(16)$$

Fig. 10 illustrates Eqs. (15) and (16). Round marks in the figure which indicate the positions of the experimental results except Pts. 4 and 5 drop close to the theoretical curve.

Table 4 Positions of the peak at the identical time.

θ	Experiment Δt (s)	Experiment r(cm)	Theory Δt (s)	Theory r (cm)
0	0	15	0	15
$-\pi/2$	0.00184	10.1	0.00129	11.6
$-\pi$	0.00280	7.5	0.00258	8.1
$-5\pi/4$	0.00126	11.6	0.00323	6.4
$-3\pi/2$	0.00153	10.9	0.00387	4.7
$-5\pi/3$	0.00432	3.3	0.00430	3.5
$-11\pi/6$	0.00514	1.3	0.00474	2.4
0	0	25	0	25
$-\pi/2$	0.00176	20.3	0.00130	21.5
$-\pi$	0.00282	17.5	0.00260	18.1
$-5\pi/4$	0.00116	21.9	0.00325	16.3
$-3\pi/2$	0.00128	21.6	0.00390	14.6
$-5\pi/3$	0.00456	12.8	0.00434	13.4
$-11\pi/6$	0.00562	10.8	0.00477	12.5

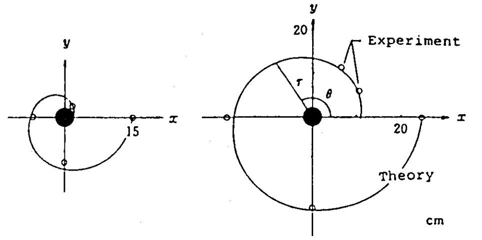

Fig. 10 Correlation between the positions of the peak and the wave front obtained by experiment and theory respectively.

5. TRANSMISSION OF VIBRATION FROM VIBRATOR TO CONCRETE AND DAMPING DURING PROPAGATION

The amplitude of acceleration at P(r,θ) is given by

$$a_m=a_0\sqrt{\frac{d}{2r}}\,e^{-\beta\left(r-\frac{d}{2}\right)} \quad \cdots\cdots(17)$$

From logarithms of Eq. (17), the following formula is obtained.

$$\ln\left(a_m/\sqrt{\frac{d}{2r}}\right)=\ln a_0-\beta\left(r-\frac{d}{2}\right) \quad \cdots\cdots(18)$$

This means that there is a linear relation between $\ln(a_m/\sqrt{d/2r})$ and $(r-d/2)$. Accordingly, the intersection of a regression line of test results and the vertical axis gives $\ln a_0$, and its gradient is $-\beta$. Thus, two parameters; a_0, β; essential and sufficient to

Table 5 Relationship between amplitude of acceleration and distance from the vibrator.

Concrete	t (s)		r−d/2 (cm) 5.4	10.4	15.4	20.4	25.4	35.4	45.4	50.4	$\ln a_0$	β (cm^{-1})	correl coeff
Plain	0	a_m	8.46	2.32	4.64	2.55	2.16	1.53	1.25	1.09	2.817	0.0236	-0.678
		u	2.79	1.75	2.62	2.14	2.08	1.89	1.81	1.72			
	5	a_m	6.67	2.50	3.03	1.57	1.37	1.31	0.83	0.87	2.293	0.0184	-0.803
		u	2.55	1.83	2.19	1.66	1.62	1.73	1.40	1.49			
	10	a_m	6.41	3.21	3.57	2.35	1.57	1.52	0.83	0.87	2.509	0.0218	-0.918
		u	2.51	2.08	2.35	2.06	1.76	1.88	1.40	1.49			
	15	a_m	6.41	3.57	4.28	2.35	1.76	1.74	1.25	0.87	2.550	0.0188	-0.872
		u	2.51	2.18	2.54	2.06	1.87	2.02	1.81	1.49			
	20	a_m	4.36	2.50	3.39	1.96	1.57	1.52	1.25	0.87	2.148	0.0098	-0.662
		u	2.13	1.83	2.30	1.88	1.76	1.88	1.81	1.49			
	25	a_m	4.87	3.21	3.21	1.96	1.57	1.52	1.25	0.87	2.271	0.0134	-0.858
		u	2.23	2.08	2.25	1.88	1.76	1.88	1.81	1.49			
	30	a_m	5.26	3.57	4.11	2.54	1.76	1.74	1.25	0.87	2.473	0.0166	-0.861
		u	2.31	2.18	2.50	2.14	1.87	2.02	1.81	1.49			
	Av.	a_m	6.06	2.99	3.75	2.18	1.68	1.55	1.13	0.90	2.422	0.0171	-0.871
		u	2.46	2.01	2.40	1.99	1.83	1.90	1.70	1.53			
			5.7	10.7	15.7	20.7	25.7	35.7	45.7	50.7			
AE	0	a_m	15.52	6.43	7.50	4.40	3.60	1.09	0.71	0.71	3.659	0.0502	-0.962
		u	3.42	2.79	3.11	2.70	2.60	1.55	1.24	1.29			
	5	a_m	15.77	5.36	6.07	4.20	3.60	3.92	1.43	1.79	3.213	0.0216	-0.791
		u	3.43	2.60	2.89	2.65	2.60	2.83	1.94	2.22			
	10	a_m	11.54	3.57	3.57	2.80	2.40	4.13	1.61	1.79	2.653	0.0091	-0.392
		u	3.12	2.20	2.36	2.24	2.19	2.89	2.06	2.22			
	15	a_m	8.72	1.91	2.14	2.40	1.20	3.70	1.43	1.79	2.066	0.0123	-0.040
		u	2.84	1.57	1.85	2.09	1.50	2.78	1.94	2.22			
	20	a_m	11.29	3.21	2.14	2.40	1.20	3.26	1.07	1.43	2.447	0.0126	-0.392
		u	3.10	2.09	1.85	2.09	1.50	2.65	1.65	1.99			
	25	a_m	11.54	2.50	1.79	2.00	1.20	3.48	1.25	1.43	2.259	0.0072	-0.211
		u	3.12	1.84	1.67	1.91	1.50	2.72	1.81	1.99			
	30	a_m	8.72	2.14	1.79	2.40	0.80	3.05	1.07	1.43	2.098	0.0056	-0.164
		u	2.84	1.69	1.67	2.09	1.09	2.58	1.65	1.99			
	Av.	a_m	11.87	3.59	3.57	2.94	2.00	3.23	1.22	2.04	2.657	0.0118	-0.467
		u	3.15	2.20	2.36	2.29	2.01	2.64	1.78	2.35			

$u=\ln(a_m/\sqrt{d/2r})$

describe the change in the amplitude of acceleration with the distance from the vibrator can be determined. Table 5 gives the results obtained by analysing the experimental data described in chapter 3. Fig. 11 shows two cases; $t=0$ and average; for ordinary and AE concretes. The ratio of transmitted acceleration a_0 to generated acceleration of vibrator a_v is defined as transmission ratio R_t, i.e. $R_t = a_0/a_v$. R_t and attenuation coefficient β are given in Table 6. Fig. 12 shows the changes of them with the time of vibration. As seen in the figure, both a_0 and β change little with the time of vibration for the ordinary concrete and the average values are 11.12 G and 0.0171 cm^{-1} respectively. While for the AE concrete, though a_0, R_t and β are greater than those for the ordinary concrete at the beginning of vibration, they decrease rapidly, in about 10 sec, to the values similar to those for the ordinary concrete.

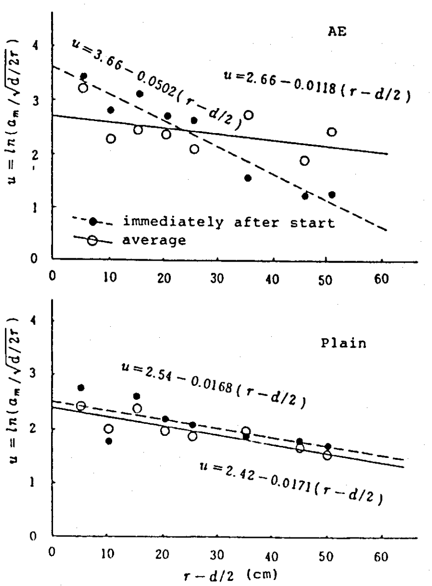

Fig. 11 Relationship between acceleration amplitude and distance from the vibrator.

Table 6 Changes in the rate of transmission of amplitude from the vibrator to fresh concrete and the attenuation constant with the time of vibration.

Concrete	t (s)	Beginning	5	10	15	20	25	30	Average
Plain	a_0 (G)	12.63	9.95	12.30	12.81	8.57	9.69	11.86	11.12
	a_v (G)	54.84	48.39	48.39	48.39	48.39	48.39	48.39	48.39
	a_0/a_v (%)	23.0	20.1	25.4	26.5	17.7	20.0	24.5	22.5
	β (cm^{-1})	0.0168	0.0188	0.0218	0.0188	0.0098	0.0134	0.0166	0.0171
AE	a_0 (G)	38.83	24.85	14.20	7.90	11.56	9.58	8.15	
	a_v (G)	59.68	51.62	51.62	48.39	48.39	48.39	48.39	
	a_0/a_v (%)	65.1	48.1	27.5	16.3	23.9	19.8	16.8	
	β (cm^{-1})	0.0502	0.0216	0.0091	0.0121	0.0126	0.0072	0.0056	

a_v : Acceleration of the vibrator

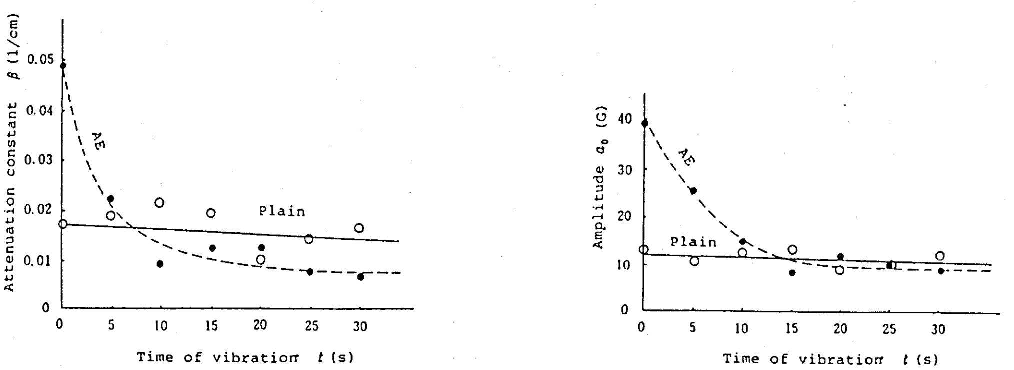

Fig. 12 Changes in acceleration amplitude at the position of vibrator surface and attenuation constant with the time of vibration.

6. THE VERIFICATION OF WAVE FUNCTION BY INTERFERENCE TESTS

To confirm the validity of Eq. (8), theoretical distribution of acceleration for combined vibration by two vibrators was calculated from Eq. (8), and visual tests were carried out. For this purpose, a twin type vibrator composed of two vibrating heads with the same characteristics exept the opposite directions of rotation of the eccentric weight axles was considered.

The origin of the coordinates is taken at the contact point of two vibrating heads, and the measurement of time is begun at the moment when the gravity centroids of the rotating axles come right on the x-axis confronting each other. If the position of point P with coordinates (r, θ) is expressed as (r_1, θ_1) from the center line of the right head O_1 and as (r_2, θ_2) from that of the left head O_2 (Fig. 13), through similar consideration as stated in chapter 2, the acceleration a_1 in the direction of θ_1 by the right head and that a_2 in the direction of θ_2 by the left head are obtained as follows.

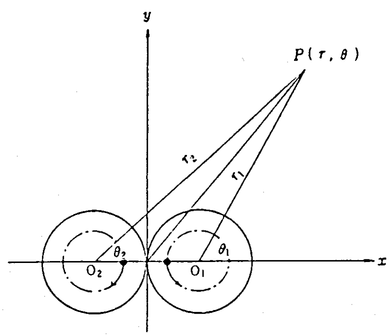

Fig. 13 Twin type vibrator.

$$a_1 = a_0\sqrt{\frac{d}{2r_1}}\, e^{-\beta\left(r_1-\frac{d}{2}\right)} \sin\left\{\omega t - \frac{\omega}{c}\left(r_1-\frac{d}{2}\right)-\theta_1\right\} \cdots\cdots\cdots\cdots (19)$$

$$a_2 = -a_0\sqrt{\frac{d}{2r_2}}\, e^{-\beta\left(r_2-\frac{d}{2}\right)} \sin\left\{\omega t - \frac{\omega}{c}\left(r_2-\frac{d}{2}\right)+\theta_2\right\} \cdots\cdots\cdots (20)$$

The magnitude of resultant acceleration is

$$a=\sqrt{(a_1\sin\theta_1+a_2\sin\theta_2)^2+(a_1\cos\theta_1+a_2\cos\theta_2)^2} \cdots\cdots\cdots (21)$$

Then, the maximum acceleration a_m will be obtained by calculating a with varying t. Here, r_1, r_2, θ_1, and θ_2 have geometrical relations with r and θ as

$$r_1=\sqrt{r^2-rd\cos\theta+\left(\frac{d}{2}\right)^2}$$

$$r_2=\sqrt{r^2+rd\cos\theta+\left(\frac{d}{2}\right)^2}$$

$$\theta_1=\sin^{-1}\left(\frac{r\sin\theta}{r_1}\right)$$

$$\theta_2=\sin^{-1}\left(\frac{r\sin\theta}{r_2}\right)$$

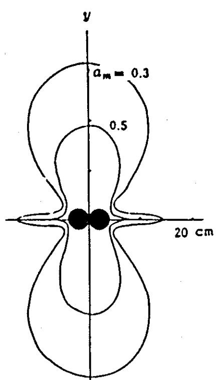

Fig. 14

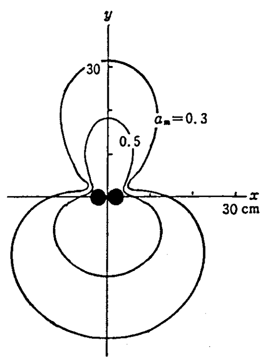

Fig. 15

Theoretical distribution of acceleration amplitude generated by twin type vibrator (a_m : relative amplitude of acceleration).

At first, these formulas were calculated for the first and second quadrants and expected Fig. 14. However, the formulas from r_1 to θ_2 have been lately revised for the rectangular coordinates so as to obtain a_m at any point P(x, y).

$$r_1=\sqrt{\left(x-\frac{d}{2}\right)^2+y^2}$$

$$r_2=\sqrt{\left(x+\frac{d}{2}\right)^2+y^2}$$

$$\theta_1=\tan^{-1}\left\{y\Big/\left(x-\frac{d}{2}\right)\right\}$$

$$\theta_2=\tan^{-1}\left\{y\Big/\left(x+\frac{d}{2}\right)\right\}$$

Fig. 15 is a result calculated by the latter formulas with the values; $a_0=1$, $d=4$ cm, $f=200$ Hz, $c=49.2$ m/sec, and $\beta=0.0171$ cm^{-1}. In order to ascertain the figure of equi-amplitude of acceleration, a twin type vibrator which had the above mentioned characteristics was produced. Its structure is as follows: It has two vibrating heads each of which contains an eccentric weight axle. These axles are connected with a driving axle by the gears so that they rotate in the opposite directions at the same speed. The vibrating heads are tightly connected at the position of the node of vibration.

Photo 1 A photograph of the surface of sand layer vibrated with the twin type vibrator.

When this vibrator was driven in fresh concrete, bleeding water was observed on the concrete surface in the shape like a figure of eight. Further, when the vibrator was operated in the saturated sand layer, water gain which was thought to be caused by the liquefaction of the sand took place, and the domain of effective vibration could be recognized more clearly than in the case of concrete. Photo 1 is one of the photographs showing the view of the surface after vibration. Though it resembles both Fig. 14 and Fig. 15, the correct result of calculation is believed to be Fig. 15, because the result for the third and fourth quadrants is the same that obtained for the first and second quadrants by substituting $-\omega$ for ω in Eqs. (19) and (20).

7. THE APPLICATION OF THE WAVE FUNCTION TO THE EFFECTS OF THE FORMS

The vibration of concrete was analysed under the influences of reflected waves from the surfaces of a rectangular form as follows. The origin of the coordinates is taken at the center line of the vibrator and the mirrored images of the origin are designated O_1, O_2, O_3, and O_4. The dimenssions of the form, the distances from point P(x, y) to the origin, mirrored points, and so forth are as shown in Fig. 16. Analysis only for the first quadrant is necessary, because the results for the other quadrants can be obtained by choosing the conditions properly. From the geometrical relations and Eq. (8) following formulas are derived.

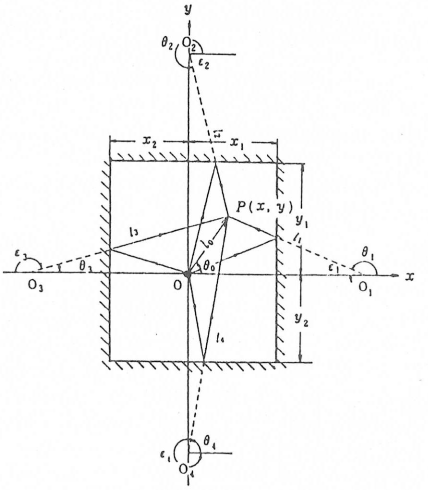

Fig. 16 Reflections of vibration at the surfaces of the form.

$$a_{p0}=a_0\sqrt{\frac{d}{2\,l_0}}\,e^{-\beta\left(l_0-\frac{d}{2}\right)}\sin\left\{\omega t-\frac{\omega}{c}\left(l_0-\frac{d}{2}\right)-\varepsilon_0\right\}\quad\cdots\cdots(22)$$

$$a_{pi}=R_r a_0\sqrt{\frac{d}{2\,l_i}}\,e^{-\beta\left(l_i-\frac{d}{2}\right)}\sin\left\{\omega t-\frac{\omega}{c}\left(l_i-\frac{d}{2}\right)-\varepsilon_i\right\}\quad\cdots\cdots(23)$$

in which $i=1, 2, 3, 4$; R_r=reflection coefficient, and

$$\varepsilon_1=\tan^{-1}\left(\frac{y}{2x_1-x}\right),\quad \varepsilon_2=\tan^{-1}\left(\frac{2y_1-y}{x}\right)$$

$$\varepsilon_3=\pi-\tan^{-1}\left(\frac{y}{2x_2+x}\right),\quad \varepsilon_4=2\pi-\tan^{-1}\left(\frac{2y_2+y}{x}\right)$$

$$l_0=\overline{\mathrm{OP}}=\sqrt{x^2+y^2},\quad l_1=\overline{\mathrm{O_1P}}=\sqrt{(2x_1-x)^2+y^2}$$

$$l_2=\overline{\mathrm{O_2P}}=\sqrt{x^2+(2y_1-y)},\quad l_3=\overline{\mathrm{O_3P}}=\sqrt{(2x_2+x)^2+y^2}$$

$$l_4=\overline{\mathrm{O_4P}}=\sqrt{x^2+(2y_2+y)^2}$$

$$\theta_0=\tan^{-1}\frac{y}{x}=\varepsilon_0$$

$$\theta_1=\pi-\varepsilon_1,\quad \theta_2=2\pi-\varepsilon_2,\quad \theta_3=\pi-\varepsilon_3,\quad \theta_4=2\pi-\varepsilon_4$$

Then, the magnitude of resultant acceleration is given by

$$a_p=\sqrt{\left(\sum_{i=0}^{4} a_{pi}\sin\theta_i\right)^2+\left(\sum_{i=0}^{4} a_{pi}\cos\theta_i\right)^2} \quad \cdots\cdots(24)$$

Taking i=0, 1, and y=0, then the distribution of resultant acceleration along the x-axis under the influence of a form plate is determined by

$$a_{p0}=a_0\sqrt{\frac{d}{2x}}\,e^{-\beta\left(x-\frac{d}{2}\right)}\sin\left\{\omega t-\frac{\omega}{c}\left(x-\frac{d}{2}\right)\right\}$$

$$a_{p1}=R_r a_0\sqrt{\frac{d}{2(2x_1-x)}}\,e^{-\beta\left(2x_1-x-\frac{d}{2}\right)}\sin\left\{\omega t-\frac{\omega}{c}\left(2x_1-x-\frac{d}{2}\right)-\pi\right\}$$

$$a_p=a_{p0}+a_{p1}$$

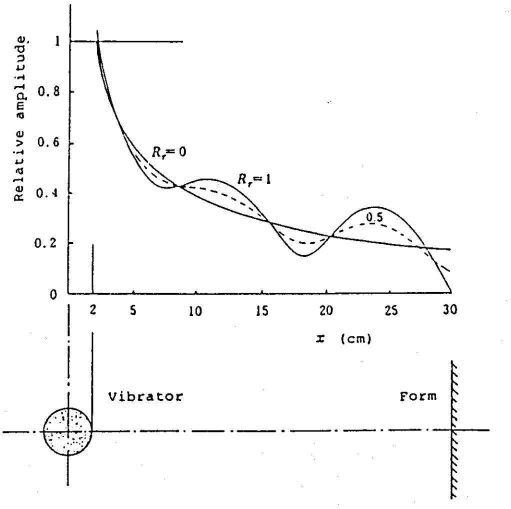

Fig. 17 Theoretical distribution of the relative amplitude of acceleration with and without effects of reflection (R_r : reflection coefficient).

Fig. 17 is an illustration of the results calculated with the values a_0=1 (in that case, a_p means a relative amplitude of acceleration), d=4 cm, $\omega=2\pi f=400\pi s^{-1}$, c=48 m/sec, β=0.0171 cm^{-1}, x_1=30 cm, R_r=0, 0.5, and 1. According to this figure, in case that the effect of reflection is prominent, the vibration will be weakened at the form surface and the place about $c/2f$ distant from the form, while intensified at the places about $c/4f$ and $3c/4f$.

8. CONCLUSIONS

A wave function has been proposed to represent the vibration which is transmitted from the internal vibrator into the fresh concrete and propagates two-dimensionally in it. A series of the vibratory experiments conducted under different conditions established the validity of this function. Further, its applicability to the analysis of the combined vibration generated by plural vibrators as well as the effect of reflection has been suggested.

The velocity of wave of propagation included in the proposed function can be estimated from the density and air content of the concrete by the formula deduced for the longitudinal wave in the fluid containing air bubbles. The frequency of vibration will scarecely decrease during propagation. The amplitude of displacement or acceleration is reduced by transmission from the vibrator and propagation in theconcrete. The parameters necessary to predict the distribution of acceleration; transmission ratio and attenuation coefficient can be determined by such means of analysing two-dimensional test results as proposed in this paper. Thus, when the informations about a minimun acceleration required to the consolidation of the concrete is available, the radius of effective action of the vibrator can be predicted. The values of transmission ratio and attenuation coefficient obtained in this research arerespectively 0.225 and 0.0171 cm^{-1} for the tested ordinary concrete. For the AE concrete they are greater than those for the ordinary concrete at the beginning of vibration, but decrease with the time of vibration to similar values.

According to the analysis of the effect of a form, the vibration is weakened at the form surface and the place about $c/2f$ distant from it, while intensified at the places about $c/4f$ and $3c/4f$. The degree of the effect depends on the reflection coefficient. Further studies on the influences of the form and vertical reinforcing bars are to be performed.

Refereces

(1) BERGSTROM Sven G., Laboratory tests on vibration of concrete, Journal of ACI, Vol. 24, No. 10, June 1953

(2) KAMIYAMA Susumu, ENDO Hiroyuki, Propagation of pressure in lightweight aggregate concrete during compaction by internal vibrator, Journal of the Society of Materials Science Japan, Vol. 18, No. 185, Feb. 1969

(3) MURATA Jiro, KAWASAKI Michio, SEKI Shiro, Behavior of concrete in consolidation by vibration, Proceedings of JSCE Symposium on the Properties of Fresh Concrete and their Application in Concreting Practice, March 1986

(4) FORSSBLAD Lars, Investigation of internal vibration of concrete, Acta Polytechnica Scandinavica, Stockholm, Civil Engineering and Building Construction Series, No. 29, 1965